

## Possible Origin of the Damocloids: the Scattered Disk or a New Region?

S. Wang<sup>1</sup>, H. B. Zhao<sup>1</sup>, J. H. Ji<sup>1</sup>, S. Jin<sup>1,2</sup>, Y. Xia<sup>1</sup>, H. Lu<sup>1</sup>, M. Wang<sup>1</sup> and J. S. Yao<sup>1</sup>

<sup>1</sup> Purple Mountain Observatory, Chinese Academy of Sciences, Nanjing 210008, China;  
jjjh@pmo.ac.cn

<sup>2</sup> Graduate School of Chinese Academy of Sciences, Beijing 100049, China

**Abstract** The Damocloids are a group of unusual asteroids, recently enrolling a new member of 2010 EJ104. The dynamical evolution for the Damocloids may uncover a connection passage from the Main Belt, the Kuiper Belt and the scattered disk beyond. According to our simulations, two regions may be considered as possible origin of the Damocloids: the scattered disk, or a part of Oort cloud which will be perturbed to a transient region locating between 700 AU and 1000 AU. Based on the potential origin, the Damocloids can be classified into two types, with relation to their semi-major axes, and about 65.5% Damocloids is classified into type I which mainly originate from Oort cloud. Whether the Damocloids is inactive nuclei of Halley Family Comets may rely on their origin.

**Key words:** methods: numerical - celestial mechanics - minor planets, asteroids: Damocloids

### 1 INTRODUCTION

In our solar system, most asteroids are classified into following types: I) Main Belt asteroids, near-earth objects and Jupiter trojans, mostly reside in the inner solar system; II) Centaurs mainly travel in the outer solar system between the regime of Jupiter and Neptune; III) Trans-Neptune objects are at or beyond the orbit of Neptune, e.g., Neptune trojans, Kuiper Belt objects and scattered disk objects. Different from asteroids, there are comets which have visible signs of outgassing in the solar system, containing Jupiter-family comets (JFCs) and Halley-family comets (HFCs). JFCs are in short periods less than 20 years, crossing Jupiter's orbit and dynamically dominated by major planets (Duncan 2008). HFCs are comets with orbital periods between 20~200 years, with perihelion distances less than 1.5 AU (Bailey & Emel'yanenko 1996).

To date, there are many other small bodies which cannot be catalogued into the aforementioned types, e.g., 1998 WU24 ( $e = 0.9, q = 1.4$  AU) (Davies et al. 2001) and 1999 LD31 ( $e = 0.90, q = 2.38$  AU) (Harris et al. 2001), both moving on an eccentric orbit. Both of them share similar orbits with HFCs, without visible signs of outgassing. According to their common properties, these bodies now belong to a new population - the Damocloids (Jewitt 2005).

The Damocloids are objects which have a Tisserand Parameter with respect to Jupiter not larger than 2 (Jewitt 2005). The Tisserand Parameter is expressed as,

$$T_J = \frac{a_J}{a} + 2\left[(1 - e^2)\frac{a}{a_J}\right]^{1/2} \cos i, \quad (1)$$

where  $a_J$ ,  $a$ ,  $e$ ,  $i$  refer to the semi-major axis of Jupiter, the semi-major axis, eccentricity and inclination of the small body, respectively. According to the definition, there are 77 Damocloid candidates,

consisting of 41 Damocloids with decent orbits up to 2011 February. The Tisserand Parameter is always used to distinguish the JFCs and HFCs and other asteroids in the solar system. For JFCs, we have  $2 < T_J < 3$ ; while for HFCs we have  $T_J < 2$ , which is also the criteria for the Damocloids. But for other asteroids, one may obtain  $T_J > 3$ .

On March 10, 2010, we discovered a new asteroid moving along a very eccentric orbit, designated as 2010 EJ104. We observed this rapidly moving object using 1.04/1.20 m Schmidt Telescope (Near Earth Object Survey Telescope) at Xuyi station of Purple Mountain Observatory (PMO) (Zhao et al. 2008, Zhao et al. 2009, Zhao 2010). The orbital elements are then determined by utilizing follow-up measurements from several observatories – the semi-major axis  $a = 21.58$  AU, eccentricity  $e = 0.90$ , and inclination  $i = 41.55^\circ$ , perihelion distance  $q = 2.13$  AU. The orbital elements and their  $1\sigma$  uncertainties are shown in Table 1. The orbital feature shows that this object is similar to 1998 WU24 and 1999 LD31 (Davies et al. 2001, Harris et al. 2001). On the basis of the orbital data, the Tisserand Parameter for 2010 EJ104 is about 1.568. Additionally, the object is similar to other members of the Damocloids, which are also no cometary feature. Hence, the Damocloids now enroll a new member of 2010 EJ104, with a total number up to 42.

Then a natural question may be raised – where does the Damocloids come from and is there a source or region that may replenish these comparable objects? As they have similar orbital properties with HFCs, if they arise from same source, or in other words, are the Damocloids the inactive nuclei of HFCs? Nowadays, several scenarios have been proposed to shed light on possible dynamical origin for such objects.

Firstly, minor objects in the inner solar system could be scattered out due to severe perturbations by giant planets (e.g., Jupiter and Neptune) during the secular evolution in the planetesimal disks (Raymond et al. 2004, Ji et al. 2005, Ji et al. 2011). For example, the trans-Neptunian objects could undergo the process of being scattered inward by Neptune (Levison et al. 2009, Moro-Martín 2008). The trans-Neptunian objects is currently postulated to originate from the Kuiper Belt and scattered disk (Gladman 2005, Morbidelli & Levison 2004). Recently, the dust disk in the Kuiper Belt may also serve as an alternate origin for these objects. Additionally, the nearby region of Jupiter may be considered as the birthplace of such objects, where  $\sim 8\%$  objects residing the orbit between Jupiter and 3.3 AU are ejected to an eccentric orbit in the simulations (Weissman & Levison 1997).

Secondly, the objects in the outer solar system that could be perturbed by passing massive stars or tidal effect of the Galactic disk. In the early 1950's, a spherical cloud, consist of numerous comets ranging from 2,000 AU to 50,000 AU, was firstly postulated to mark up the distant barrier of the solar system (Oort 1950, Weissman 1990, Dones et al. 2004), which was known as so-called Oort Cloud. Generally speaking, the Sun and major planets play insignificant part in bringing about such bodies due to their faraway distance. However, the orbital stirring arising from the passing stars or massive planets are quite significant (Morbidelli et al. 2008, Levison et al. 2004) and the tidal effects exerted by the disk (Fouchard et al. 2006) and bulge of the Milky Way may still play a very important part in producing these small bodies (Byl 1990). Suffering from complicated dynamical process, the objects in the Oort cloud will be greatly excited and further driven to be thrown into the inner solar system over longer timescale of evolution.

Recently, an alternative mechanism was proposed to explain the origin of small objects. In this scenario, a hypothetical Sun's companion (Matese & Whitmire 2011), with a mass of several Jovian masses wandering about the innermost region of the outer Oort cloud, may induce the detached Kuiper Belt objects to migrate inward and then cross over the disk, and eventually close approach the Sun. Consequently, the companion may probably trigger transportation of the objects like the Damocloids.

According to close similarity, the Damocloids may be inactive nuclei of HFCs (Jewitt 2005, Toth 2006) with same origin, while there are two main sources of HFCs: the scattered disk (Levison et al. 2006) and the inner Oort cloud (Levison et al. 2001) locating from 2000 AU to 20000 AU. Under the gravitational effect of the Sun, eight planets, passing stars, and Galactic tides, with proper distribution of inclination about  $50^\circ$ , the inner Oort cloud objects are stirred up to give birth to HFCs. According to the scattered disk model, it may predict that the number of the HFCs will be

roughly 10 times of the currently observed results, and the possible outer boundary of the scattered disk is about 200 AU.

In this Paper, we extensively study a general origin of the Damocloids through numerical simulations. And we find a transient disk locating from 700 AU to 1000 AU. Before the object become a Damocloids, it may pass through this region. In *Section2*, we briefly introduce the method, to numerically investigate the dynamical origin of the Damocloids. Next, we analyze simulation results and discuss the origin mechanisms in *Section3*, and we summarize the outcomes in *Section4*.

**Table 1** Heliocentric ecliptical orbital elements of 2010 EJ104 for TDB epoch 2455400.5 (Reference frame is ICRF/J2000)

Elements	Values	Uncertainty
$a$ (AU)	21.586266636538866	5.688461074865734E-2
$e$	0.9011439847926949	2.5546023114618503E-4
$i$ (deg)	41.551986960824294	3.1068112777202545E-3
peri (deg)	177.04115294493582	7.3861295389317065E-3
node (deg)	353.0291168885478	3.357376430876397E-4
$t_P$ (JD)	2455271.4918569964	1.7166562491213885E-2
$M$ (deg)	1.2678120987288926	4.901376431292673E-3
$q$ (AU)	2.1339323028906296	1.1173156970862058E-4

## 2 METHODS

To better understand the possible dynamical origin of the Damocloids, we investigate the past motion of them by tracing back the orbits under the perturbation of the main planets in the solar system. Backwards integration will illustrate the orbit before the Damocloids moving to the position that we observed. Herein we carry out the backwards numerical simulations in a heliocentric system using a hybrid symplectic algorithm in the MERCURY package (Chambers 1999).

We carry out 29 runs with the 29 target objects shown in Figure 1 from the Damocloids family including 2010 EJ104. In order to derive the original orbit, we create a swarm of test particles around each target object with their nominal orbital element values we observed. The initial semi-major axes, eccentricities and inclinations of the test particles are induced randomly in the range of the element uncertainties. In addition, the other initial orbital elements of each test particle are randomly generated - the arguments of periastron, longitudes of the ascending node, and mean anomalies range from  $0^\circ$  to  $360^\circ$ . For each run, we integrate backwards over the timescale of  $10^8$  years. Additionally, the hybrid integrator parameters are adopted as a stepsize of 6 days, a Bulirsch-Stoer tolerance of  $10^{-12}$ . In all runs, the gravitational interaction of the Sun and eight major planets in the solar system are fully taken into account during the integration. We stop the calculations when the test particles reach the distance from the central star larger than 1000 AU which is out of the perturbation of the inner solar system (mainly the effect of the eight major planets and the sun). On the other hand, when the test particle run into the distance closer than the radius of the sun, we assume that it collide with the sun.

At the end of the simulation, we record the information when one of the conditions is satisfied: I) the orbit of the test particle is changed into hyperbolic; II) the distance from the test particle to the sun is larger than 1000 AU; III) the distance from the test particle to the sun is closer than the radius of the sun. Above three conditions are probably caused by the reasons following, I) perturbation from the main planets in the solar system; II) escaping from the inner solar system (here we define  $d < 1000$  AU as the inner solar system,  $d$  means the distance from the central star); III) glancing from the sun. Thus, from analysis the record, we will get the possible origin of the Damocloids.

## 3 THE SCENARIO OF ORIGIN

Now we come to the simulation results. We analysis the results taking 2010 EJ104 as an example. Figure 2 shows a typical run of 2010 EJ104. In this run, the initial parameters are adopted from Table

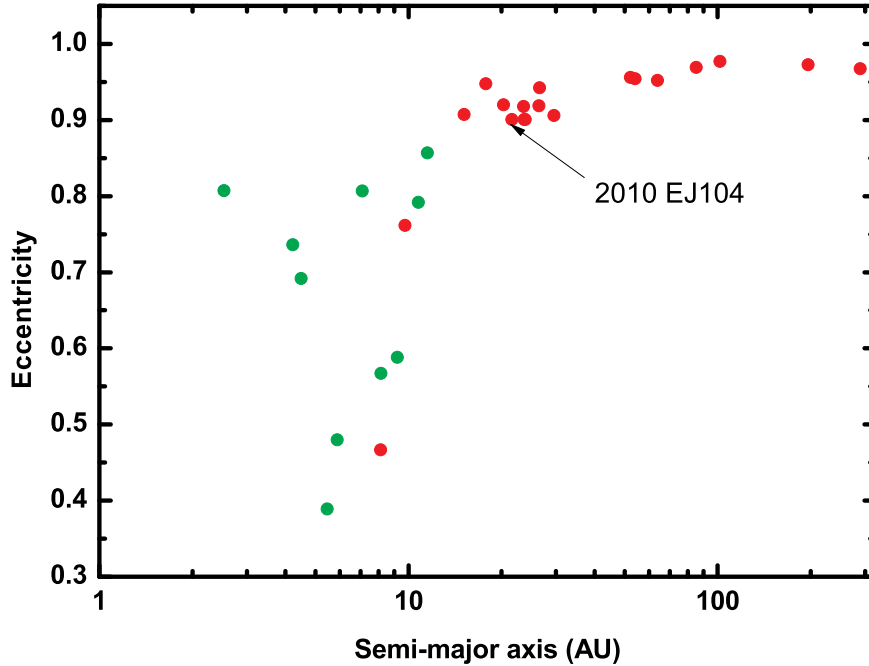


**Fig. 1** The semi-major axis versus eccentricity distribution of 29 Damocloids, where 2010 EJ104 is marked out in the figure. According to their possible origin, 29 Damocloids can be classified into four types: Type I and II are labeled in red, pink, yellow and green, respectively.

1. Eventually, the orbit of this object changes to hyperbolic with a dynamical timescale of  $\sim 2$  Myr at  $\sim 600$  AU, where it may originate from.

Figure 3 shows the orbit information of each test particle for 2010 EJ104 at the end of the simulation. From panel (a) of this figure, it can be noticed that most of test particles in our simulations run back to mainly two regions – the disk at a distance within 300 AU away from the Sun (labeled Region I) or a disk between 700 AU and 1000 AU (labeled Region II). Analysis the results, we find that, Region I is mainly composed by two kinds of test particles. One’s orbits has been changed into hyperbolic at the end of the simulation as shown in panel (b) of figure 3 and another collides with the sun in the backward simulation. While the test particles in Region II are almost the ones which escaped from the inner solar system with  $d > 1000$  AU at last, the distribution of such test particles are shown in panel (c). Thus, there are two kinds of test particles in Region I. Considering the hyperbolic orbit at the end of the simulation, One part may be involved in the scattering scenario due to stirring by major planets when it lies in the scattered disk (Duncan & levison 1997) or the Main Belt, especially the scattered disk will encounter Neptune during the dynamical evolution in solar system (Gladman 2005). Another part is those that may be originated from the glancing of the sun. 37% test particles in Region I.

The objects in Region II will escape to the outer solar system further than 1000 AU if we continue our calculation. Thus the objects in Region II may be attributed to Oort cloud by three mechanisms as aforementioned: the first one is the influence of a passing star or massive planets (Morbidelli et al. 2008), the second mechanism is the induced tidal effect by the galactic disk (Fouchard et al. 2006), and the third

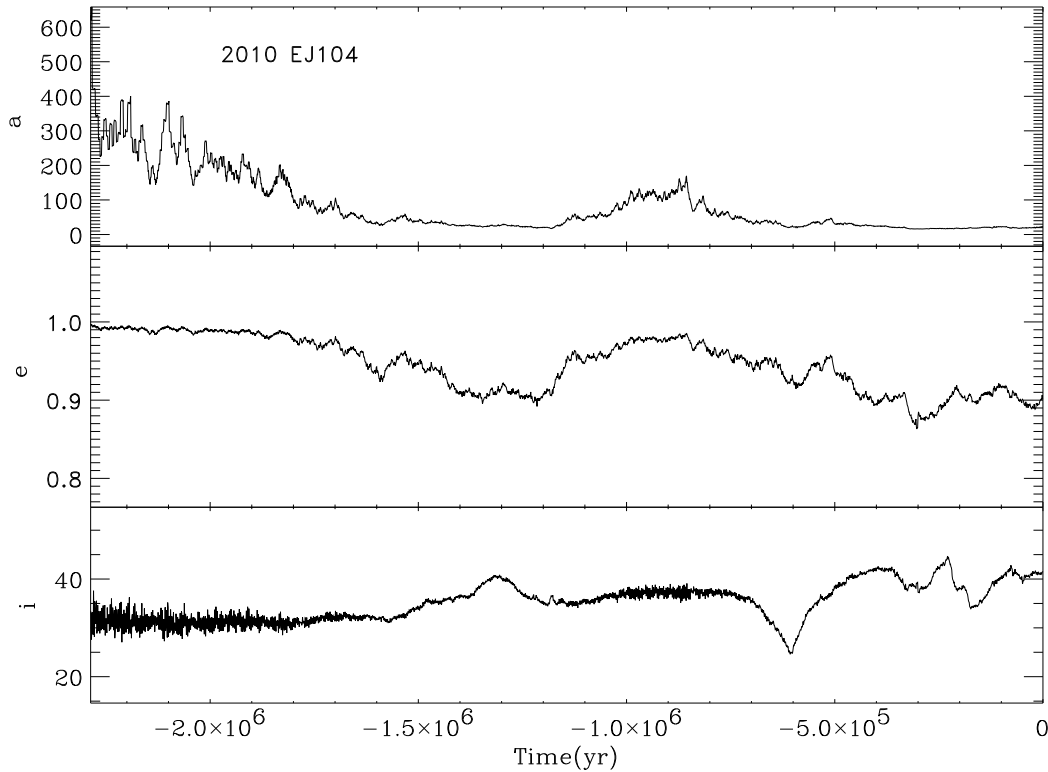


**Fig. 2** The orbit of 2010 EJ104 is integrated backwards about 2 Myr. Three panels shows the dynamical evolution of its semi-major axis  $a$ , eccentricity  $e$  and inclination  $i$ , respectively. At the end of the simulation, the object transfers to hyperbolic orbit at  $\sim 600$  AU.

scenario may result from the perturbation of the solar companion (Matese & Whitmire 2011). Although only the Galactic tides cannot bring the objects from the inner Oort cloud to the locations below  $10^3$  AU, about 70% of them with small perihelion can be brought to inner region of solar system due to the perturbation of the main giant planets (Levison et al. 2001). From the results of Levison et al. 2001, if the object in the inner Oort cloud with the perihelion distance around the locations of the main giant planets in the solar system, gravitational encounters with the giant planets cause random walk in semimajor axis. If semimajor axis decreases to about 30 AU, outer giant planet will hand off it to the inner giant planet and finally scatter it into the inner solar system. If semimajor axis increases to distance larger than 15000 AU, the effect of Galactic tide becomes significant and will take the object to a orbit with few hundreds AU semimajor axis and small perihelion distance. Another evolution process, a passing star can lower the perihelion distance of the object in the inner Oort cloud to the inside of Jupiter's orbit. Then the interaction with Jupiter will make it to the region locating from 700 AU to 1000 AU. Figure 13 of their paper shows four kinds of evolution processes from the inner Oort cloud to the inner solar system. Figure 4 in our paper shows the semimajor axes and perihelion distances results of all the objects that run back to Region II at the end of the simulations. In order to explain our results clearly, we change our results to barycentric system in figure 4 and 5. The perihelion distances shown by the green points in figure 4 are mostly range from 1 AU to 10 AU where can be perturbed by the main planets. Figure 5 shows a typical evolution process. The red line, blue line, and the black line represent the evolution of the semimajor axis, the perihelion distance, and the barycentric distance respectively. The grey dot lines

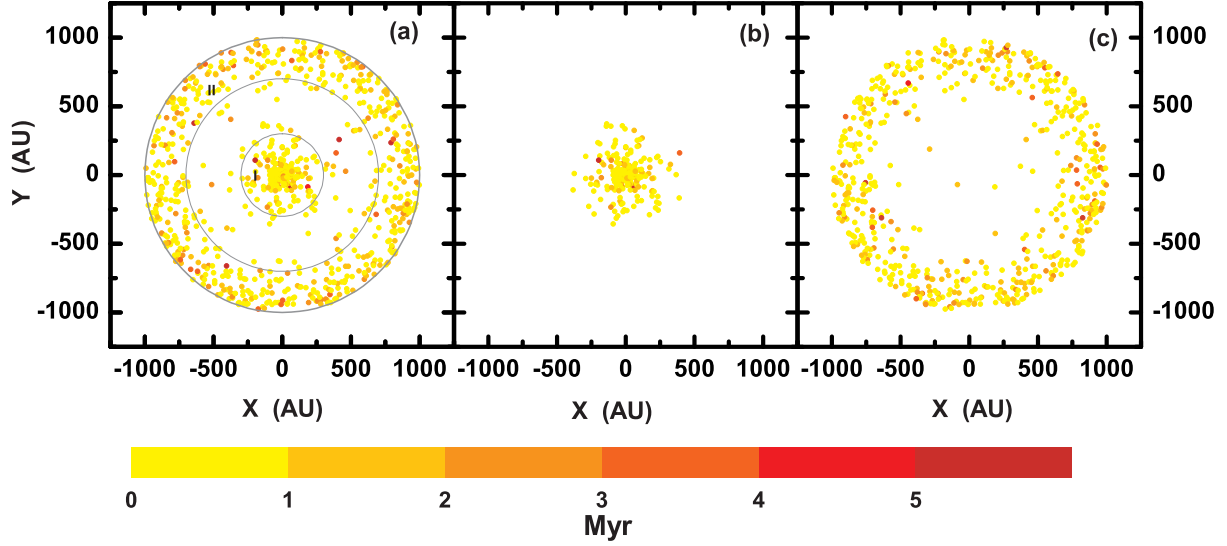


**Fig. 3** Results of backward simulations. Based on observational uncertainties, all test bodies are initially set to be  $21.586 \pm 0.057$  AU. In the figure, all of bodies had been tracked for their birthplace. The bodies from the disk within 300 AU is marked up as Region I (the outer belt), while those from 700 ~ 1000 AU are labeled Region II (inside the innermost circle). The average lifetime of all bodies is about  $9.93 \times 10^5$  years, where deeper color index indicates longer lifetime. Panel (b) shows the test particles whose orbits changed into hyperbolic or collide with the sun. Panel (c) shows the test particles which escaped from the inner solar system.

display the location of the main planets from Mars to Neptune. The object runs back to the barycentric distance about  $10^3$  AU. The forthcoming evolution process can be described as follows. Firstly, object from the inner Oort cloud is perturbed to the Region II. Then close encounter with Neptune will hand off the object to Saturn and in turn to Jupiter. Finally interacting with Jupiter makes it a Damocloids. According to this formation scenario, before object which come from Oort cloud become Damocloids, it must transit the disk. From the statistic result, 63% test particles run back to Region II.

We make an analysis over other 28 groups of simulations and find that the Damocloids mainly run back to two regions as shown in Figure 3. We show our results in Table 2. A represents the number of the test particles running back to Region II, while B displays that in Region I. C and D illustrate the number of the test particles that perturbed by the main planets and the sun respectively. Thus  $B = C + D$  is satisfied. The last column in Table 2 exhibits the ratio of the number in Region I and Region II. In order to clearly illustrate the results, we define three new parameters:  $f_{\text{RegionI}}$ ,  $f_{\text{RegionII}}$  means the probability of the Damocloids from Region I and II, respectively, and  $f$  is expressed as

$$f = \frac{f_{\text{RegionI}}}{f_{\text{RegionII}}}. \quad (2)$$

From the results in Table 2 and the definition of  $f$ , the Damocloids can be further categorized into two types.

(1) Type I:  $f < 1$ . Similar to the case of 2010 EJ104, over 50% of the test particles run back to Region II. It means that the perturbation from Oort cloud is the main reason for the formation of this type of Damocloids. 19 of 29 Damocloids could be grouped into Type I, which are labeled in red in Figure 1.

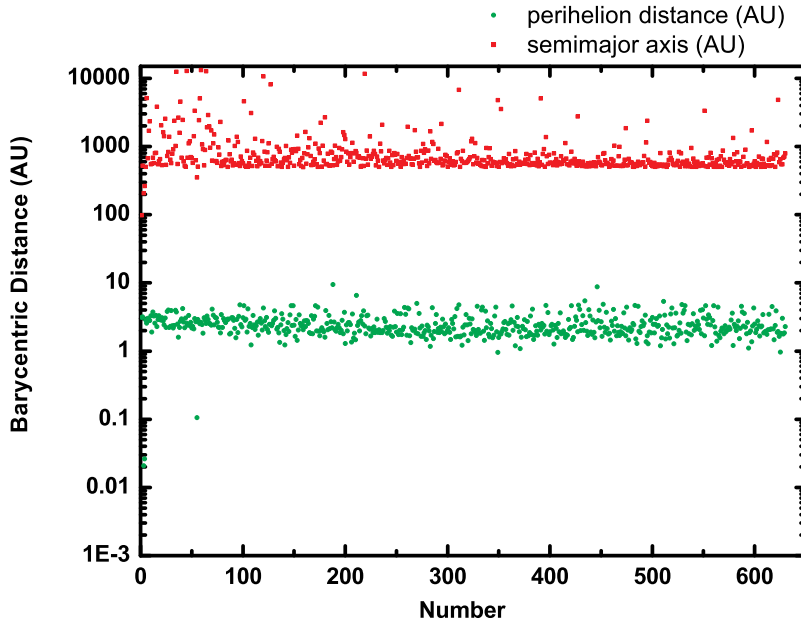


**Fig.4** Statistic results of the objects which run back to Region II in the simulation of 2010 EJ104. The red filled squares mean the semimajor axes and the green points represent the perihelion distance. The grey dot lines display the location of the main planets from Mars to Neptune.

(2) Type II:  $f > 1$ . Different from type I, perturbation in the inner solar system including the effect of the eight major planets and the sun lead to the formation of Damocloids. While, the scattered disk may be the most possible origin of the Damocloids. Ten Damocloids in our samples are contained in this type, where are marked up in green in Figure 1.

From the color of dots in Figure 1, we notice that Type I and II have apparently marked off a boundary at about 15 AU. Based on the statistic results over 29 Damocloids, the average possibility of the Damocloids population originating from Region I and II are about 65.5% and 34.5%, respectively.

As mentioned in the first section, the HFCs are mainly from two possible regions, the scattered disk or the inner Oort cloud. According to our results, the Damocloids may come from two regions too, the scattered disk or the Oort cloud which will be perturbed into the transient disk locating from 700 AU to 1000 AU. In this sense, the same origin may imply the Damocloids may be the inactive nuclei of the HFCs. In future with more carefully investigation will get the detailed results.

#### 4 CONCLUSIONS AND DISCUSSIONS

On the basis of the overall dynamical analysis, we underline that two regions are likely to serve as birthplace for the Damocloids, the scattered disk inside 100 AU (response to Region I) and Oort cloud (respond to Region II). According to their possible origin, they can be further classified into two types: Type I indicates that the objects mainly come from the Oort cloud which respond to the backward orbit to Region II; Type II suggests the population is mostly from the scattered disk which will be perturbed by the major planets or the sun.

In this work, we did not consider the effect of the outer solar system. Thus, the evolution in the region with the distance from the central star larger than 1000 AU is not clear. If the Damocloids come from inner Oort cloud, we may briefly summarize the possible routes for such objects: firstly, the bodies in Oort cloud might be stirred by perturbation of the passing stars or the tidal effect by the Galactic disk,

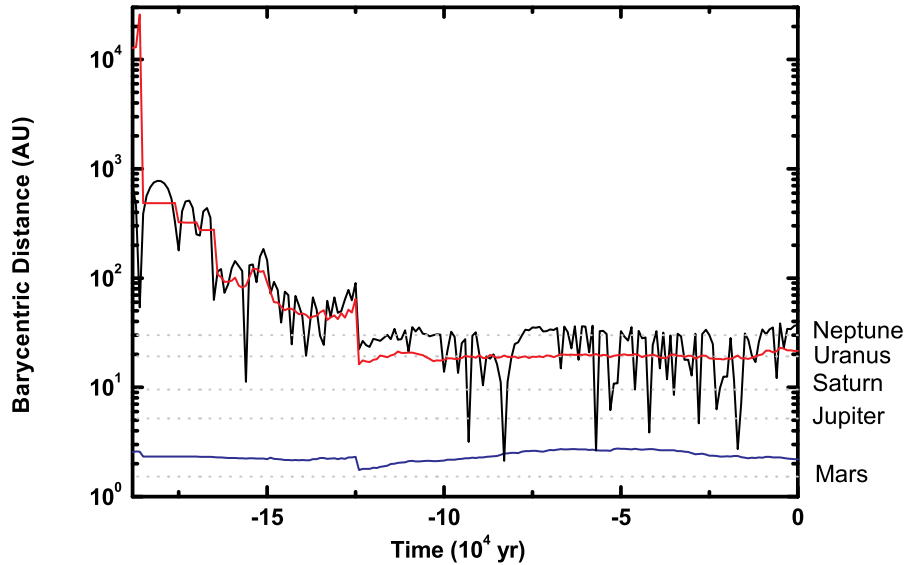


**Fig. 5** Typical result of the object which run back to Region II. The red line means the evolution of semimajor axis, blue line represents the perihelion distance and the black line shows the evolution of the barycentric distance.

then continuously moved inward to the intermediate region (Region II), and finally ejected into the inner solar system.

Additionally, the outer asteroid belt is another possible origin of Damocloids. Bodies removed from this region are found to fall under the gravitational influence of Jupiter that scatters them to large heliocentric distance (Fernandez et al. 2002). It is then possible that some scattered asteroids can return as Damocloids.

In this paper we only study the origin of the Damocloids from the point of backward simulations. Thus, scattered disk and inner Oort cloud are just two possible origins of Damocloids. But still there are other possible origins such as the asteroid belt including the main belt and the outer belt. It will be much elucidated for their origin with more members of Damocloids observed in future.

**Acknowledgements** We thank Zhaori Getu, Hong Renquan and Hu Longfei who have greatly contributed to the asteroid survey observation. Z.H.B is supported by the National Natural Science Foundation of China (Grants No. 10503013, 10933004), J.J.H is grateful to the support by the National Natural Science Foundation of China (Grants 10973044, 10833001), the Natural Science Foundation of Jiangsu Province, and the Foundation of Minor Planets of Purple Mountain Observatory.

## References

- Bailey, M. E., & Emel'yanenko, V. V., 1996, *MNRAS*, 278, 1087  
 Byl, J. 1990, *AJ*, 99, 1632  
 Chambers, J. E. 1999, *MNRAS*, 304, 793  
 Davies, J. K., et al., 2001, *Icarus*, 150, 69  
 Dones, L., Weissman, P., Levison, H. F., & Duncan, M. 2004, in *Comets II*, ed. M. C. Festou, H. U. Keller, & H. A. Weaver (Tucson: Univ. Arizona), 153



**Table 2** Statistic results of the Damocloids. A represents the number of the test particles that escaped from the inner solar system; B displays the number of the test particles that perturbed by the main planets or the sun; C means the number of the test particles that perturbed by the main planets and D means the number of the test particles that perturbed by the sun. Therefore,  $B = C + D$ . The value of  $f$  is got from equation 2.

Name	A	B	C	D	f
2010 NV1	923	77	77	0	0.083
2010 GW147	897	103	103	0	0.115
2004 NN8	891	109	109	0	0.122
2010 JH124	809	191	174	17	0.236
2002 RP120	746	254	245	9	0.340
2000 AB229	731	269	250	19	0.368
2000 HE46	717	283	277	6	0.395
2005 OE	713	287	256	31	0.403
1999 LD31	712	288	280	8	0.404
1997 MD10	695	305	266	39	0.439
2010 OM101	662	338	320	18	0.511
2010 EJ104	630	370	346	24	0.587
2009 YS6	625	375	353	22	0.600
2009 AU16	621	379	344	35	0.610
1998 WU24	601	399	344	55	0.664
2006 RJ2	588	412	390	22	0.701
1999 LE31	573	427	419	8	0.745
1999 XS35	571	429	392	37	0.751
2005 SB223	562	438	389	49	0.779
2000 DG8	427	573	516	57	1.342
2005 TJ50	412	588	513	75	1.427
2004 YH32	387	613	490	123	1.584
2005 NP82	353	647	535	112	1.833
2006 VW266	282	781	557	161	2.546
2009 FW23	243	757	599	158	3.115
2010 LG61	228	772	581	191	3.386
2010 OA101	154	846	541	305	5.494
2007 VA85	126	874	674	200	6.937
2009 HC82	60	940	807	133	15.667

Duncan, M. J., & Levison, H. F. 1997, *Science*, 276, 1670

Duncan, M. J. 2008, *SSRv*, 138, 109

Fernandez, J. A., Gallardo, T. & Brunini, A. 2002, *Icarus*, 159, 358.

Fouchard, M. et al. 2006, *CeMDA*, 95, 299

Gladman, B. 2005, *Science*, 307, 71

Harries, A. W. et al., 2001, *Icarus*, 153, 332

Jewitt, D. 2005, *AJ*, 129, 530

Ji, J. H., Liu, L., Kinoshita, H., & Li, G. Y. 2005, *ApJ*, 631, 1191

Ji, J. H., Jin, S., & Tinney, C. G. 2011, *ApJ*, 727, L5

Levison, H. F., Dones, L., & Duncan, M. J., 2001, *AJ*, 121, 2253

Levison, H. F., Morbidelli, A., & Dones, L., 2004, *AJ*, 128, 2553

Levison, H. F. 2006, *Icarus*, 184, 619

Levison, H. F., Bottke, W. F., Gounelle, M., Morbidelli, A., Nesvorný, D., & Tsiganis, K. 2009, *Nature*, 460, 364

Matese, J. J., & Whittemire, D. P., 2011, *Icarus*, 211, 926

Morbidelli, A., & Levison, H. F. 2004, *AJ*, 128, 2564

Morbidelli, A., Levison, H.F., & Gomes, R. 2008, *The Solar System Beyond Neptune*, 275

Moro-Martín, A. 2008, *Proceedings of IAU Symposium No. 249*, 347

- Oort, J. H. 1950, *Bull. Astron. Inst. Netherlands*, 11, 91
- Raymond S. N., Quinn T., & Lunine J. I., 2004, *Icarus*, 168, 1
- Toth, I. 2006, *Proceedings of IAU Symposium No. 229*, 67
- Weissman, P. R. 1990, *Nature*, 344, 825
- Weissman, P. R., & Levison, H. 1997, *ApJ*, 488, L133
- Zhao, H. B., Yao, J. et al. 2008, *Proceedings of IAU Symposium No. 248*, 565
- Zhao, H. B., Lu, H., Zhaori, G. T, et al. 2009, *Science in China Series G: Physics, Mechanics & Astronomy*, 52, 1790
- Zhao, H. B. 2010, *Acta Astronomica Sinica*, 51, 324